Hindawi
Advances in Materials Science and Engineering
Volume 2019, Article ID 3531543, 13 pages
https://doi.org/10.1155/2019/3531543

Research Article

Effect of Temperature and pH on Early Hydration Rate and Apparent Activation Energy of Alkali-Activated Slag

Ping Li,[1] **Jianhui Tang**,[1] **Xudong Chen**,[1] **Yin Bai**,[2] **and Qiyao Li**[1]

[1]*College of Civil and Transportation Engineering, Hohai University, No. 1 XiKang Road, Nanjing 210098, China*
[2]*Nanjing Hydraulic Research Institute, State Key Laboratory of Hydrology-Water Resources and Hydraulic Engineering, No. 34 Hujuguan, Nanjing 210029, China*

Correspondence should be addressed to Jianhui Tang; tangjianhui1994@163.com

Received 5 November 2018; Accepted 28 January 2019; Published 25 February 2019

Academic Editor: Luigi Nicolais

In order to investigate the effect of temperature and pH on the early hydration rate of alkali-activated slag (AAS), NaOH was used as alkali activator, and the nonevaporable water (NEW) content of the slag paste at different temperatures (5, 20 and 35°C) and pH (12.10, 12.55, 13.02, and 13.58) was measured. On the basis of the Arrhenius formula, the hydration rate of slag was characterized by the content of nonevaporative water, and the apparent activation energy of slag hydration at different pH was also obtained. The early hydration rate of slag was significantly affected by temperature and pH of activator solution. The apparent activation energy E_a of slag decreased with the increase of pH, and there was a good linear relationship between them. When pH was less than 13.02, increasing the temperature can accelerate the hydration rate of slag. However, under the condition of high pH (pH = 13.58), the hydration rate of slag was negatively correlated with temperature, which was related to the "shell forming" phenomenon of slag hydration.

1. Introduction

Alkali-activated cementitious materials are considered as a kind of sustainable development building materials with low carbon dioxide emission, which can be produced by industrial by-products. As a by-product of iron-making process, granulated blast furnace slag (GBFS) has become one of the most widely used materials to study the properties of alkali activated materials because of its potential cementitious properties [1–3]. Therefore, many properties of alkali-activated slag (AAS), such as activation mode of slag activity, hydration products, and mechanical properties, have been comprehensively understood [4–7]. However, the hydration of AAS is a complex dynamic process. The hydration kinetics of slag are influenced by many factors; the most important factors are the pH of the activator solution and the temperature at the time of the slag reaction.

The hydration rate (reaction degree) of slag is a key point in the study of the hydration kinetics of AAS. The related research shows that the pH of the solution plays an important role in the hydration process of the slag. The slag can be activated only in a solution of pH > 11.5 [8], and the slag hydration reaction is accelerated as the pH of the activator solution increases [9, 10]. Zhou et al. [11] used different pH values of water glass to study the kinetics of slag hydration. The results show that the higher the pH value of the water glass, the shorter the induction period of slag hydration and the faster the rate of heat evolution. Gebregziabiher et al. [12] also found that by increasing the amount of activator, the heat of hydration evolution increased. However, in the solution with high alkali concentration, a reaction shell will be formed on the surface of slag particles, which will inhibit the hydration reaction of slag in the later stage. In addition, the effect of temperature changes on the hydration reaction of AAS is also significant. Low temperature will prolong the AAS initial setting time [13], and an increase in the hydration temperature can significantly accelerate the rate of heat evolution and raise the reaction degree of AAS [14, 15], but the late strength will be reduced when the temperature exceeds 80°C [16].

Apparent activation energy, like the hydration rate, can be used to characterize the sensitivity of the AAS hydration rate to temperature changes. In the quantitative relationship between temperature and chemical reaction rate, the classical Arrhenius formula is produced [17], which is suitable for most reactions [18, 19]. The concept of activation energy in the Arrhenius formula is based on chemical elementary reactions that represent the minimum energy required for a chemical reaction to star [20]. However, the hydration of AAS is a complex reaction, including the fracture of Si-O and Ca-O bonds on the surface of slag particles and the formation of hydrated calcium silicate and hydrotalcite [21, 22], so the classical concept of activation energy is no longer applicable. Therefore, some hydration characteristics of AAS are used to determine the activation energy, namely, the apparent activation energy, which is more suitable for describing the influence of temperature on the slag hydration rate. Poole et al. [20] studied the effects of supplementary cementitious materials on apparent activation energy of cements by isothermal conduction calorimeter. It was found that an increase in apparent activation energy was observed when cement was substituted with ground granulated blast furnace slag. The same result was obtained by Barnett et al. [23]. Fernández-Jiménez and Puertas [24] investigated the influence of activator solution concentration on hydration kinetics of AAS. Their results showed that activation energy of the slag does not vary practically with the activator solution concentration. However, there is no literature about the effect of the pH of activator solution on the apparent activation energy of AAS.

The usual method for determining apparent activation energy is to measure isothermal calorimetric data [24–26] or strength [23, 27] of cementitious materials. The former method can reflect the chemical mechanism, but the testing time of the hydration heat is short, and the determination of the total hydration heat is difficult, especially at low temperature, so it is not suitable to describe the effect of temperature on the long age of the rate of hydration. It is convenient to use the strength method, but the early strength of cementitious materials develops slowly or even has no strength at low temperature, which has a great influence on the results. For cementitious materials with the same hydration products, the nonevaporative water (NEW) content represents the quantity of hydrates and degree of hydration [28, 29]. It overcomes the shortcomings of the strength method and can reflect the long-term hydration characteristics of slag, which is suitable for long-term testing [30]. Therefore, the apparent activation energy is determined by the NEW content in this study.

At present, most of the research is based on cement-based materials. But the hydration mechanism of AAS is different from that of cement, and its hydration kinetics characteristics are also different [31]. Furthermore, there is still no detailed quantitative understanding of the parameters affecting the rate of slag reaction. Therefore, in this paper, the coupled effects of temperature and pH on the hydration kinetics of the AAS were investigated by measuring the nonevaporable water content of AAS paste. The apparent activation energies of different pH values were determined by the Arrhenius formula and the temperature sensitivity of the slag hydration in different pH solutions were analyzed, which provides guidance for the application of AAS.

2. Materials and Experimental Methods

2.1. Materials. Grade S95 ground granulated blast furnace slag (GGBFS) according to GB/T 18046-2008 was used in this experiment, whose Blaine surface area was 400 m^2/kg. The chemical composition of GGBFS is shown in Table 1. The alkali activator used was sodium hydroxide (NaOH), and the deionized water was used for the preparation of different alkali solutions of pH (12.10, 12.55, 13.02, and 13.58).

2.2. Experimental Methods

2.2.1. Sample Preparation. The AAS paste was prepared by mixing GGBFS and prepared NaOH solutions; the ratios of water-to-slag (w/s) were 0.4, 0.5, and 0.6, respectively. The AAS paste was placed in disposable plastic cups for NEW content test and microscopic analysis. Above prepared samples were sealed with the plastic wrap to prevent the evaporation of water and then placed in the curing tank immediately with curing temperatures of 5°C, 20°C, and 35°C, respectively, for 1, 3, 7, and 14 days.

The samples in the plastic cup that has been cured to the specified ages were taken out, broken into small pieces of about 2 mm, and ground in a mortar to pass through the 0.075 mm square hole sieve. The samples were covered with the anhydrous ethanol during the grinding process. After the end of the grinding, the samples were immersed in absolute ethanol for 24 hours to terminate the hydration. The samples were then filtered and dried at 105°C for 2 hours. The dried samples were ground again in a mortar to disperse the agglomerated sample during the drying process and then placed in a desiccator for later testing.

2.2.2. Testing. The content of NEW was measured by the method of high temperature furnace burning [11]. The dry sample was weighed about 1 g (accurate to 0.0001 g) with an analytical balance. The sample is put into a crucible that has been burnt to constant quantity. Then, the crucible is placed in a high temperature furnace. The temperature in the furnace is gradually increased to about 950 ± 25°C and burned for 15 min to 20 min. After the end of the heating, the crucible was taken out and placed in a desiccator, cooled to room temperature, and weighed. Repeat the burning until constant weight. The nonevaporable water content was calculated according to the following formula:

$$N = \left[\frac{(M_1 - M_2)(100 - L)}{M_2}\right] - L\,(\%), \quad (1)$$

where N is the nonevaporable water content (%), M_1 and M_2 are the masses of the samples before and after the

Table 1: The chemical composition of GGBFS.

Chemical composition	CaO	SiO_2	Al_2O_3	MgO	SO_3	TiO_2	Na_2O	Fe_2O_3	K_2O	MnO	LOI
Wt (%)	39.38	32.03	15.46	8.42	1.14	1.02	0.49	0.45	0.36	0.18	0.8

calcination, respectively (g), and L is the loss on ignition of the initial slag (%).

The complete hydration sample of AAS was prepared by placing the slag in the 1 mol/L NaOH solution at curing temperature of 35°C for three months. During the period, the hardened slag paste was crushed and ground several times and the NaOH solution was added continuously so that the slag was always immersed in the solution. By measuring the NEW content of the complete hydrated sample, the ultimate nonevaporated water content (N_u) was obtained, which was basically stable at 19.97%. The microstructure of the hydration product on the surface of slag particles was observed with a Hitachi S4800 scanning electron microscope (SEM).

3. Results and Discussion

3.1. Nonevaporable Water (NEW). The variation of the NEW content of AAS paste with pH at different hydration ages is shown in Figure 1 for three w/s values at different curing temperatures. As expected, the NEW content at the same temperature depended on the pH of solution, which increased with the increase of pH of solution. In the solution of pH ≤ 13.02, the content of NEW increased with the increase of hydration temperature during the testing ages. However, when the pH of the solution was higher than 13.02, the NEW content revealed a different change with the temperature and age. In the solution of pH 13.58, the NEW content of AAS pastes with different w/s values cured at 20°C was always greater than that at 35°C throughout the hydration age. However, this phenomenon is not applicable to AAS paste with solution pH less than 13.58. In addition, the NEW content at 5°C exceeded that at 35°C after 3 days. Moreover, it reached the maximum after 7 days. The higher the content of the NEW, the more the hydrated products. That is to say, the AAS produced more hydration products at 5°C than at 35°C. This phenomenon is related to the "shelling" characteristics of alkali-activated slag hydration and will be discussed later. In addition, by comparing the different w/s, it is found that as the w/s increased, the NEW content of the AAS paste also increased [30].

3.2. The Hydration Degree of Slag. It is important to determine the hydration degree of slag for studying the reaction kinetics of AAS, evaluating the reactivity of slag and the application of slag. In the study of the NEW content of the ordinary Portland cement, it is found that the NEW content is about 22% [32], and the NEW content has a strong linear relationship with the degree of hydration [29]. Therefore, in this study, the hydration degrees of slag paste under different hydration conditions were calculated based on the content of NEW. The calculation formula is as follows:

$$\alpha(t) = \frac{N(t)}{N_u}, \tag{2}$$

where $N(t)$ is the NEW content (%) of slag paste at the hydration age t (day), N_u is ultimate NEW content (%), and $\alpha(t)$ is the degree of hydration at the hydration age t. According to equation (2), the hydration degree of AAS pastes with a w/s of 0.4 was calculated, and the hydration degree changes with the curing age at different temperatures and pH are shown in Figure 2.

It can be seen that temperature and pH have a great influence on the hydration process of AAS. At 5°C, the hydration degree of the slag in the pH ≤ 13.02 solution changed slowly and steadily with the age, and the highest degree of hydration was only 5.6%. This indicates that the diffusion rate of OH^- is slowed down at low temperature, and the collision ability with the slag particles is weakened so that the activation time of slag activity is prolonged and the hydration degree increases slowly. While in the solution of pH 13.58, the hydration degree of slag reached 22.7% at 1 day and increased with curing age. Although the slag is still at the low temperature, the pH value of the solution increases, that is, the concentration of OH^- in the solution increases, which greatly increases the collision probability between the OH^- and the slag particles. So, the activation time of the slag activity is greatly shortened and the hydration degree increases rapidly.

At 20°C, in the solution with pH of 12.10 and 12.55, the hydration degree of slag firstly increased slowly and then showed a sudden increase after 7 days. While in the solution of pH 13.58, the activation time of slag activity was very short, and the degree of hydration reached 29.2% at 1 day. But when the solution pH was 13.02, it can be clearly seen that the hydration degree of slag changes with time is different from that in other pH solutions. The degree of hydration increases with the increase of curing age, and the rate of increase is faster than that of in other pH solutions after 1 day. This indicates that the hydration of slag enters the acceleration period.

When curing at 35°C, the hydration degree of the slag varying with the age in different pH solutions is almost the same. The slag activity was quickly activated at the early stage of hydration, and then the slag was continuously hydrated and the degree of hydration constantly increased. Similarly, the hydration degree of slag was the highest in the solution of pH 13.58, and the hydration degree of slag reached 26.4% at 1 day.

In addition, by comparing and analyzing the hydration degree of slag in the same pH solution at different temperatures, it is found that in the solution with pH ≤ 13.02, the

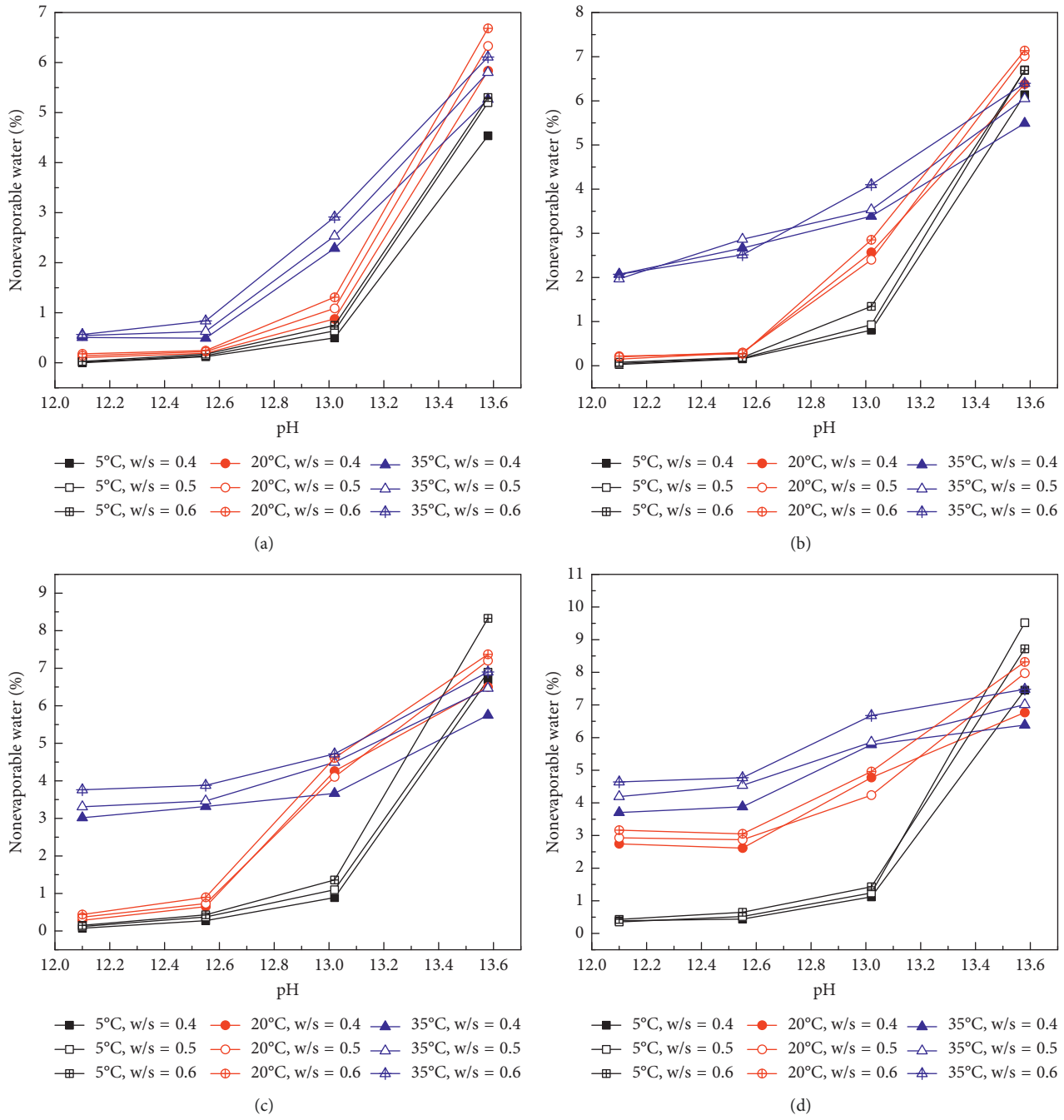

Figure 1: Variation of the NEW content of AAS paste with pH at different ages. (a) 1 day; (b) 3 days; (c) 7 days; (d) 14 days.

elevated temperature accelerates the hydration of the slag. This is because with the increase of temperature, the diffusion rate of OH ions becomes faster and the probability of interaction between OH^- and slag particles is increased, and the time of activation of slag activity is also shortened, resulting in different regularities of the degree of hydration with time. However, in the solution with pH 13.58, the degree of slag hydration with temperature and age is consistent with the law of NEW content. After 3 days of hydration, the degree of hydration at 5°C exceeded that at 35°C, which may be related to the structural differences of slag hydration products at different temperatures.

3.3. The Hydration Rate and Apparent Activation Energy. It is defined here that the ratio between the hydration degree of slag and the hydration age t is called the hydration rate of slag.

$$\beta = \frac{\alpha(t)}{t}, \tag{3}$$

where $\alpha(t)$ is the hydration degree of slag at age t; t is the hydration age; and β is the hydration rate of slag. The meaning of the hydration rate, β, reflects the growth rate of NEW content, which can be used to compare the variation of slag hydration rate with temperature and pH at different

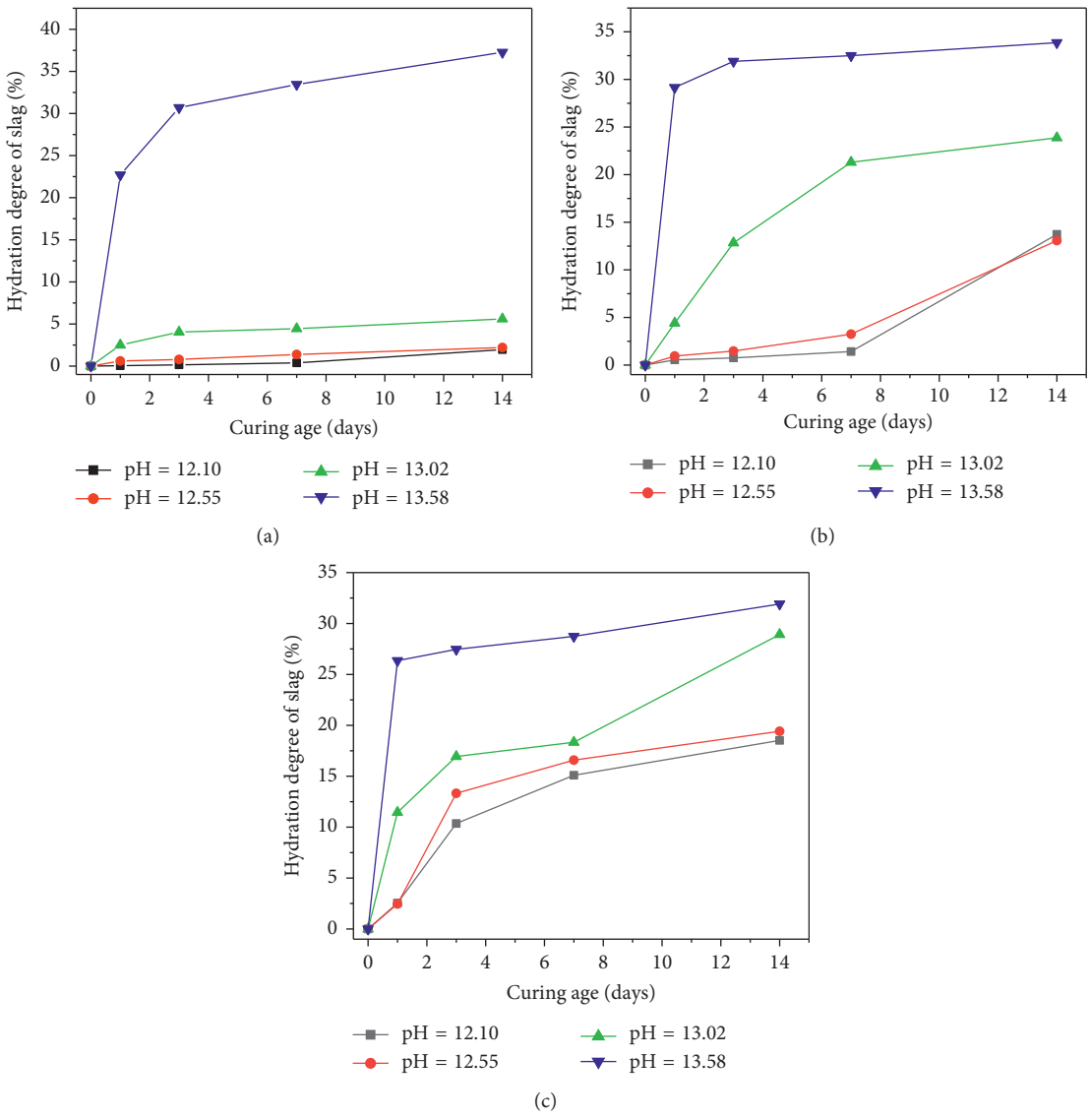

Figure 2: Water-to-slag ratio = 0.4; early hydration degree of slag changes with age at (a) 5°C, (b) 20°C, and (c) 35°C.

curing ages. This relationship can be described by the Arrhenius formula:

$$k = Ae^{-(E_a/RT)}, \tag{4}$$

$$\ln k = -\frac{E_a}{R}\frac{1}{T} + \ln A, \tag{5}$$

where R is the gas constant (8.314 J/mol/K); T is the absolute temperature (K); k is the reaction rate constant; A is the proportionality constant; and E_a is the activation energy of the reaction (J/mol). According to equation (4), the relationship between $\ln k$ and $1/T$ is linear. Therefore, the activation energy E_a can be obtained from the slope $(-(E_a/R))$ of the obtained straight line by measuring the reaction rate constant k at different temperatures.

In the Arrhenius formula, when the reactant concentration is constant, the reaction rate is proportional to the reaction rate constant. Here, the hydration rate β of the slag is regarded as the reaction rate constant k in the Arrhenius formula. According to equations (4) and (5), the relationship between the hydration rate β and the absolute temperature T is defined by

$$\beta = A_0 e^{-(E_a/RT)}, \tag{6}$$

$$\ln \beta = -\frac{E_a}{R}\frac{1}{T} + \ln A_0, \tag{7}$$

where A_0 is the proportionality constant (same units as β); R and T are the same as the above definition; and E_a is the apparent activation energy of slag hydration.

In this experiment, the hydration rate β at different temperatures is calculated by equation (3). According to equation (7), the relationship between $\ln \beta$ and $1/T$ of different ages and w/s ratios is shown in Figures 3–6. It can be seen from the figure that $\ln \beta$ and $1/T$ show a good linear relation under different ages and w/s ratios except in the

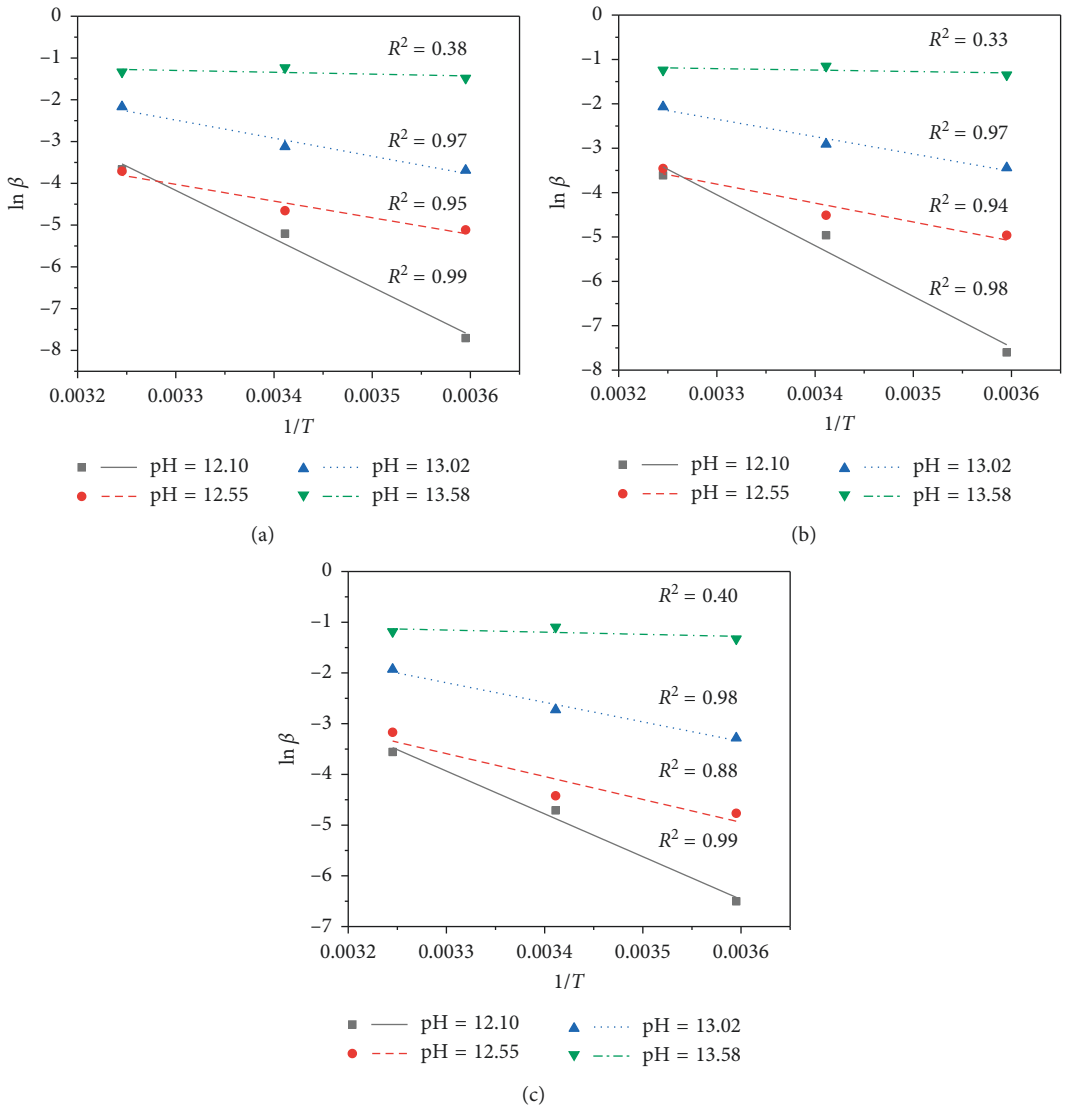

Figure 3: Effect of curing temperature on the hydration rate β at different w/s ratios for 1 day: (a) w/s = 0.4; (b) w/s = 0.5; (c) w/s = 0.6.

solution with pH 13.58. It indicates that the change of temperature T has a great influence on the early hydration rate β of AAS, and the relation between them accord with the exponential law. In the solution of pH 13.58, ln β and $1/T$ present a better linear relation after 7 days. On the contrary, compared with the other pH, the hydration rate decreases as the temperature increases.

According to the linear relationship between ln β and $1/T$, E_a is obtained by the slope of the line, as shown in Table 2. The apparent activation energy E_a varying with pH under different w/s ratios and ages is shown in Figure 7. As can be seen from Figure 7, the apparent activation energy E_a decreases as the pH of the activator solution increases, which shows a good linear relationship between them except for curing for 1 day. This may be because in the lower solution of pH (pH ≤ 13.02), the slag activity is not fully activated within 1 day, and the degree of hydration is low, resulting in a larger dispersion. Mehdizadeh and Najafi Kani [19] found that the apparent activation energy E_a of alkali-activated phosphorus slag ranged from 39.2 to 44.5 kJ/mol and increased with the increase of SiO_2/NaO_2 molar ratios in the activator solution. Zhou et al. [11] obtained the apparent activation energy E_a of 53.63 kJ/mol by using sodium silicate with pH = 13.75, while Fernández-Jiménez and Puertas [24] obtained the apparent activation energy E_a of 58.33 kJ/mol by using sodium silicate with pH = 13.20. From this, we can see that the apparent activation energies E_a obtained by scholars are different. But by comparison, it can be found that the apparent activation energy decreases with the increase of alkalinity, which is consistent with the conclusions of this paper. In addition, the w/s ratio also has a little effect on the apparent activation energy E_a. In general, as the w/s ratio increases, the apparent activation energy E_a tends to decrease. The reason is that with the increase of w/s, the collision probability between OH^- and slag particles in solution increases. Correspondingly, the rate of slag hydration is accelerated, which led to the decrease of apparent activation energy.

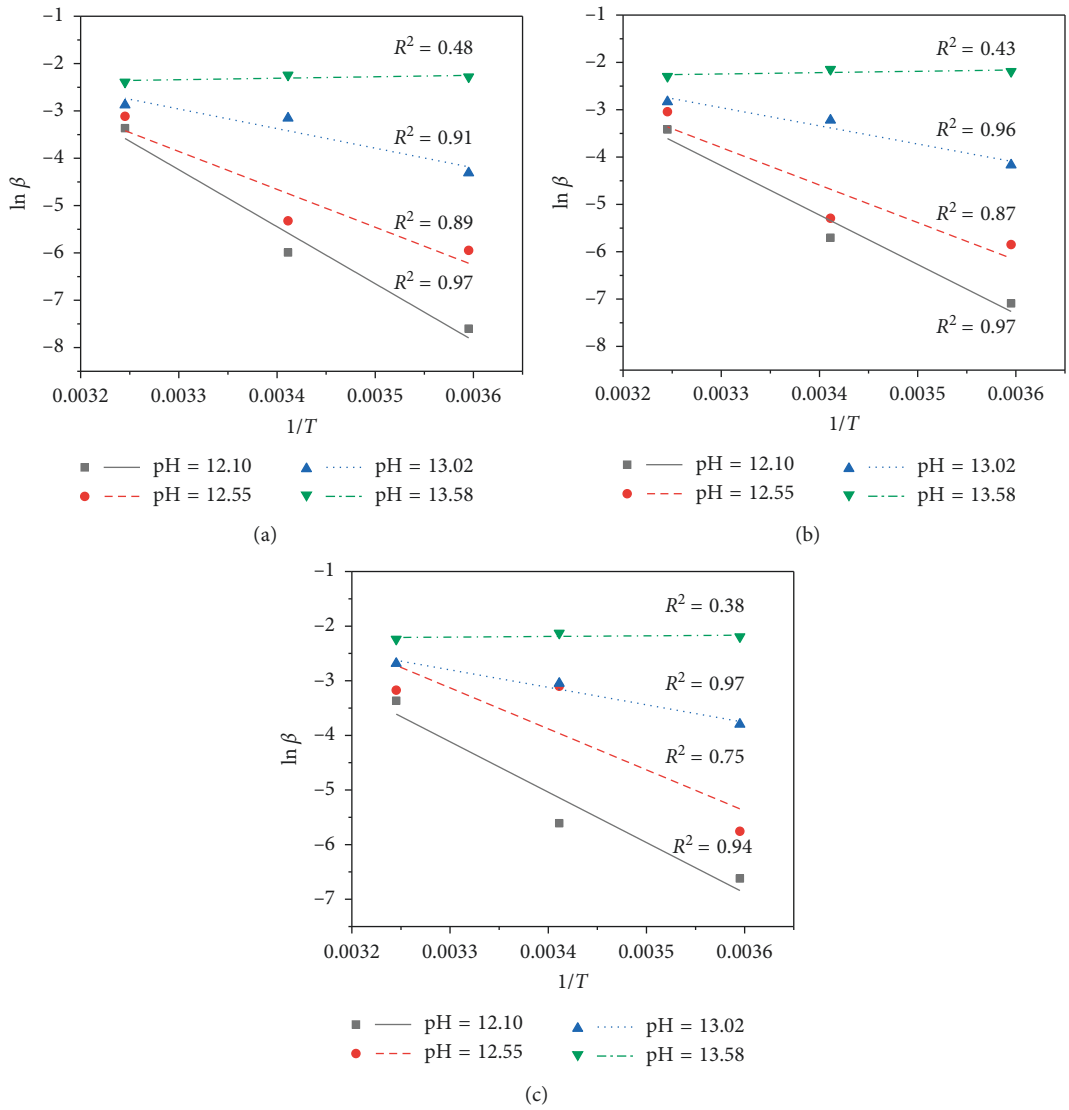

Figure 4: Effect of curing temperature on the hydration rate β at different w/s ratios for 3 days: (a) w/s = 0.4; (b) w/s = 0.5; (c) w/s = 0.6.

In the solution of pH 13.58, the calculated apparent activation energy E_a is negative value after 1 day (Table 2). This is unreasonable in the Arrhenius formula. As mentioned earlier, the apparent activation energy here is not the actual activation energy, but it can be used as a comparison between slag hydration kinetics at different pH solutions. The negative value indicates that the hydration rate in the solution of pH 13.58 at 5°C and 20°C exceeded that at 35°C. The temperature is negatively correlated with the hydration rate of slag, and increasing the hydration temperature inhibits the hydration reaction of the slag. This phenomenon is related to the "shell forming" phenomenon of slag. In the high temperature and high pH hydration environment, the slag particles will be rapidly hydrated and a hard shell is formed on the surface of its particles, which will slow down the hydration rate of the slag. This is verified in the subsequent microscopic analysis.

$\ln A_0$ is obtained by the intercept of the $\ln \beta$ and $1/T$ lines, as shown in Table 3. The change of $\ln A_0$ with pH under different w/s ratios and ages is shown in Figure 8. It can be seen that the variation of $\ln A_0$ with pH is consistent with the change of apparent activation energy with pH of solution. With the increase of pH, $\ln A_0$ decreases and there is a strong linear correlation between them. Moreover, $\ln A_0$ also shows a decreasing trend with the increase of w/s. In the Arrhenius formula, the proportionality constant A is a constant related to the collision of reactant molecules, which is affected by the concentration of reactant. Here, the proportionality constant A_0 is a constant related to the activation speed of the slag activity, which is related to the pH of the activator solution. At the same w/s, the higher the pH is, the higher the concentration of OH^- in the solution is. Therefore, the quicker the activation of slag activity is, the smaller the frequency factor A_0 is. Like the apparent activation energy, the proportionality constant A_0 appears negative value in the solution of pH 13.58. This phenomenon is consistent with the cause of the apparent activation energy, which is related to the characteristics of slag hydration.

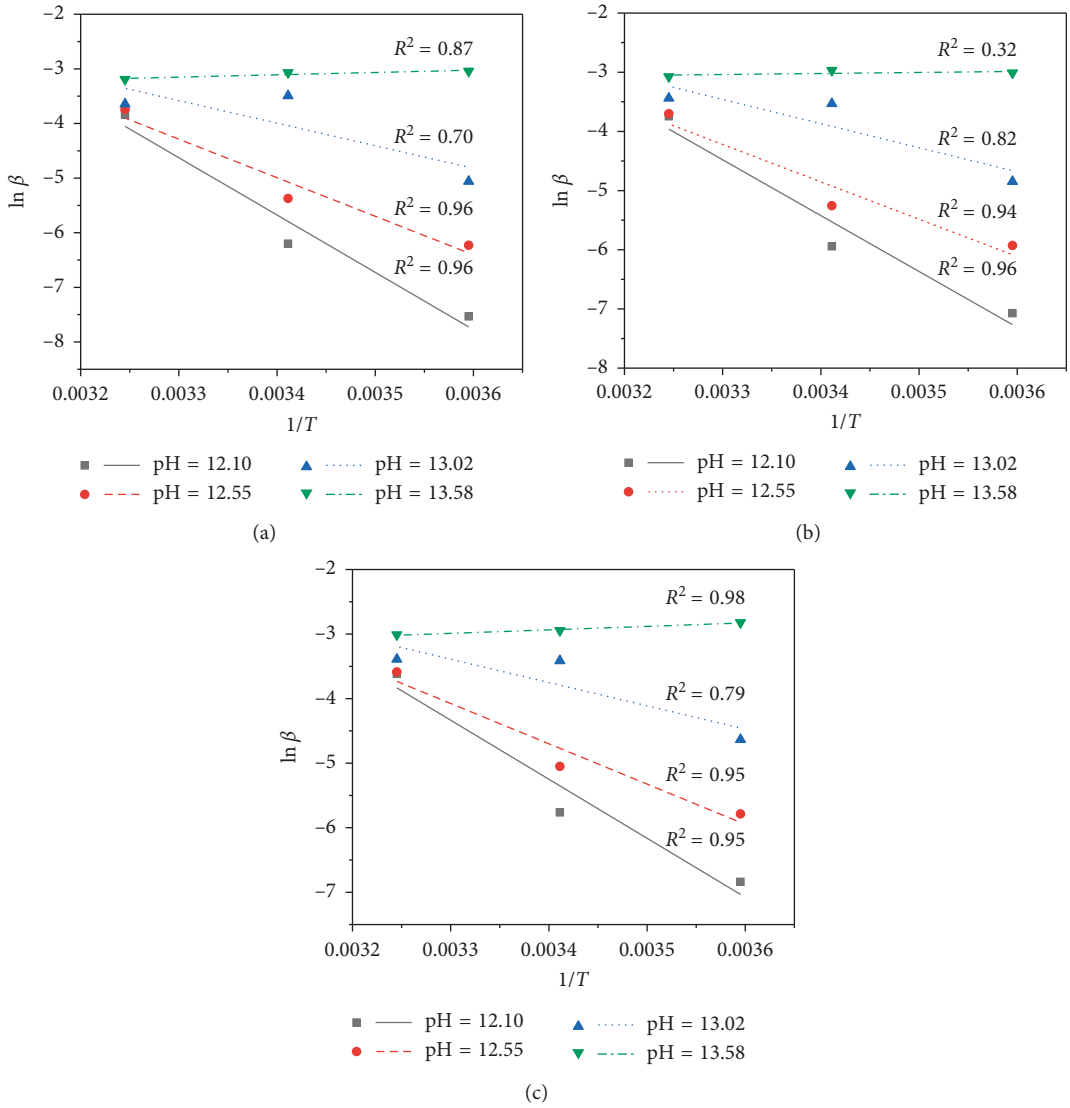

Figure 5: Effect of curing temperature on the hydration rate β at different w/s ratios for 7 days: (a) w/s = 0.4; (b) w/s = 0.5; (c) w/s = 0.6.

4. Discussion

When the Arrhenius formula is used to study the influence of temperature and pH on the hydration rate of slag, it is found that the Arrhenius formula is very suitable in the solution of pH less than 13.02. However, in the solution of pH 13.58, the ln β shows a very poor linear correlation with $1/T$ when the slag was cured at 1 day or 3 days. Moreover, they showed a negative linear correlation after 7 days. That is, as the temperature increased, the rate of hydration slowed down. In addition, the apparent activation energy E_a and proportionality constant A_0 appear negative values in the formula, which is actually related to the "shell forming" characteristics of slag hydration. The hydration reaction of slag is different from that of chemical elementary reaction. It is a complex process. In order to understand the hydration mechanism of cementitious materials more clearly, some microscopic analytical methods, such as mercury intrusion method and scanning electron microscope, are needed [30, 33, 34]. In this paper, the surface hydration characteristics of slag particles cured at 5°C and 35°C for 1 day and 14 days with the solution pH 13.58 have been observed by scanning electron microscopy (SEM), as shown in Figure 9.

As can be seen from Figure 9, when the slag was cured for 1 day, a large number of intricately connected network products appeared on the surface of the slag particles at 5°C, while the surface of the slag particles at 35°C was covered by the bulk product except for the network product. When the hydration age reached 14 days, the surface of the slag particles at 5°C was still similar to that at 1 day, but the pores of the product were finer and denser. While the surface of the slag particles at 35°C was completely surrounded by massive hydration products, which formed a hard reaction shell.

Through the above analysis, it is known that the structure of the net hydrated product formed on the surface of the slag particles at 5°C makes the OH^- in the solution permeate through the mesh and diffuse into the slag particles, which is beneficial to the further hydration of the slag. On the

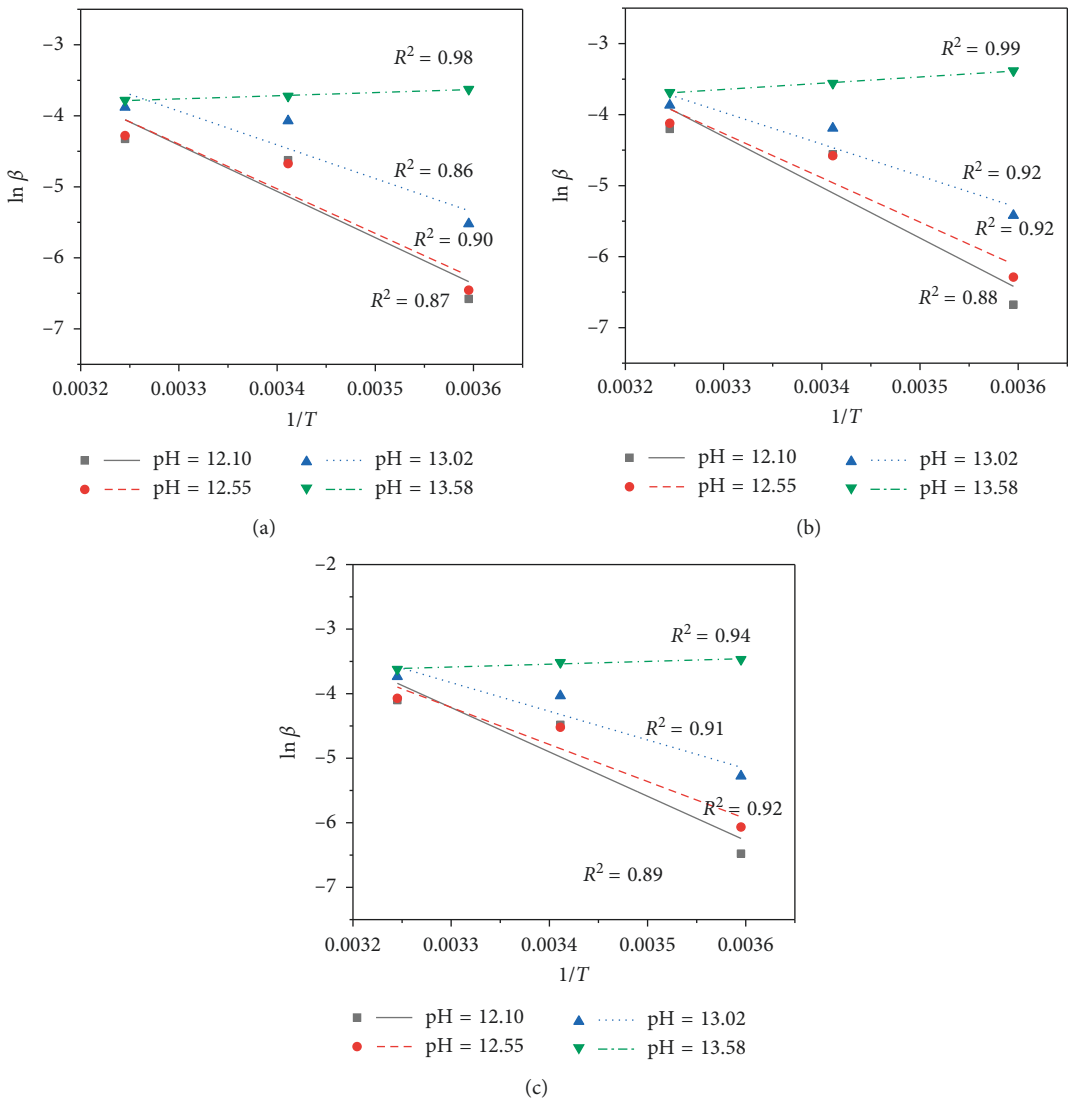

Figure 6: Effect of curing temperature on the hydration rate β at different w/s ratios for 14 days: (a) w/s = 0.4; (b) w/s = 0.5; (c) w/s = 0.6.

Table 2: Apparent activation energy E_a of slag at different pH solutions.

Curing age (day)	w/s	E_a (kJ/mol)			
		12.10	12.55	13.02	13.58
1	0.4	96.21	33.19	35.96	3.68
	0.5	95.2	35.45	32.50	2.71
	0.6	70.14	37.55	32.08	3.51
3	0.4	100.1	66.56	34.40	−2.56
	0.5	86.79	65.93	31.92	−2.35
	0.6	76.73	62.37	26.60	−0.99
7	0.4	87.26	58.69	34.34	−3.56
	0.5	78.49	52.53	33.91	−1.46
	0.6	76.03	51.91	30.01	−4.49
14	0.4	54.15	52.23	39.47	−3.70
	0.5	59.44	51.93	37.22	−7.29
	0.6	57.11	47.76	36.95	−3.61

contrary, at 35°C, the slag particles are rapidly hydrated and the early hydration degree is high. But a reacting shell is formed on the surface of the particles, which causes the OH^- to be unable to pass through the shell, so the rate of hydration also slows down. Therefore, this "shell forming" characteristic of slag hydration results in negative values of apparent activation energy E_a and ln A_0 in the solution of pH 13.58.

Taking the derivative of equation (6) with respect to T, equation (8) is obtained:

$$\frac{d \ln \beta}{dT} = \frac{E_a}{RT^2}. \tag{8}$$

Integrate equation (8) from T_1 to T_2:

$$\ln \frac{\beta_2}{\beta_1} = \frac{E_a}{R}\left(\frac{1}{T_1} - \frac{1}{T_2}\right). \tag{9}$$

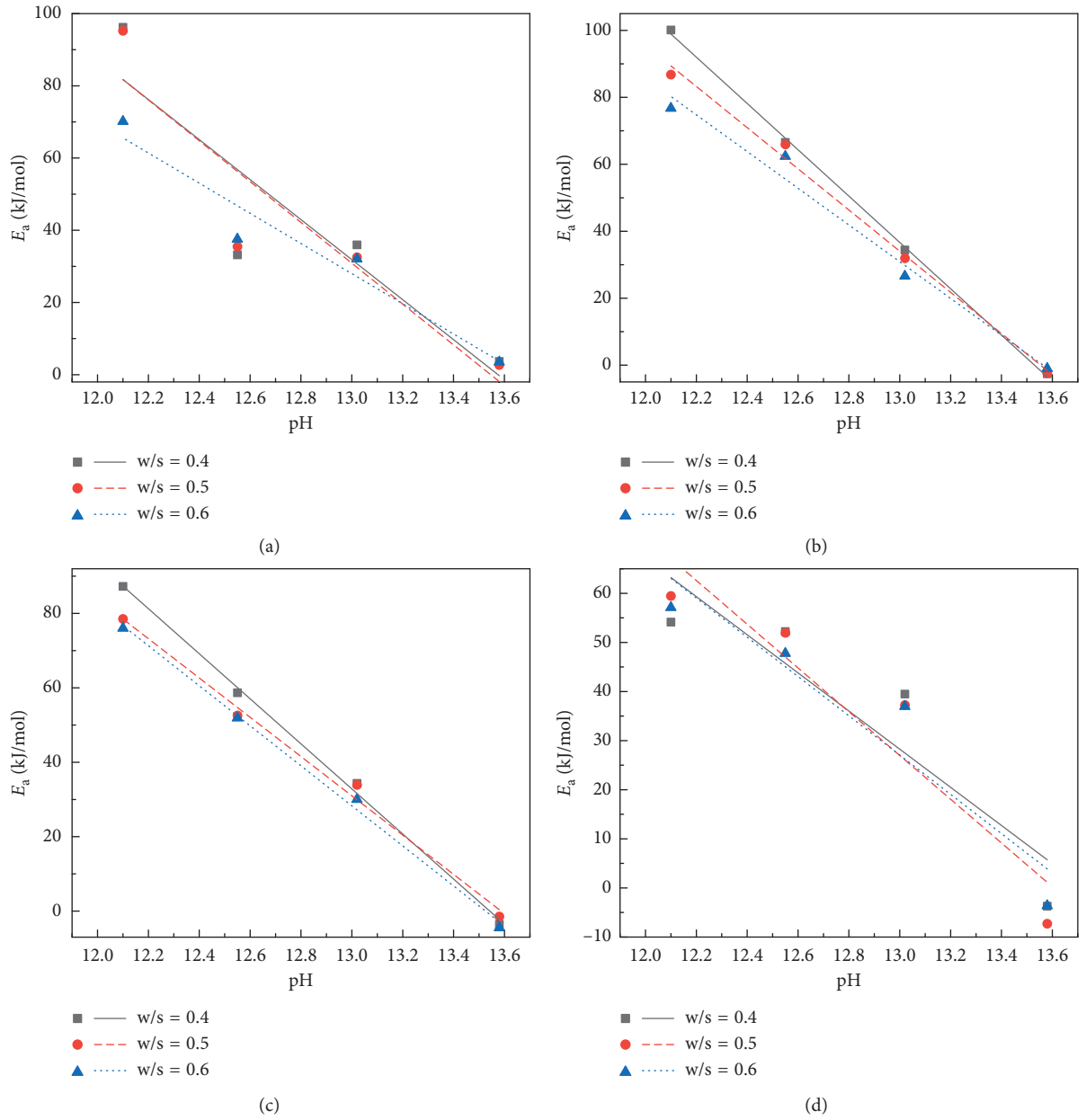

Figure 7: E_a changes with pH at (a) 1 day, (b) 3 days, (c) 7 days, and (d) 14 days.

Table 3: $\ln A_0$ at different pH solutions.

Curing age (day)	w/s	$\ln A_0$			
		12.10	12.55	13.02	13.58
1	0.4	34.016	9.1489	11.785	0.1631
	0.5	33.734	10.262	10.55	−0.1327
	0.6	23.905	11.313	10.54	0.2372
3	0.4	35.49	22.56	10.696	−3.3574
	0.5	31.366	23.468	10.811	−2.078
	0.6	26.34	21.62	7.76	−2.59
7	0.4	30.011	19.008	10.049	−4.566
	0.5	26.677	16.632	9.9992	−3.6166
	0.6	25.843	16.53	8.5206	−4.7696
14	0.4	17.082	16.332	11.733	−5.2306
	0.5	19.284	16.346	10.807	−6.5371
	0.6	18.451	14.743	10.839	−5.021

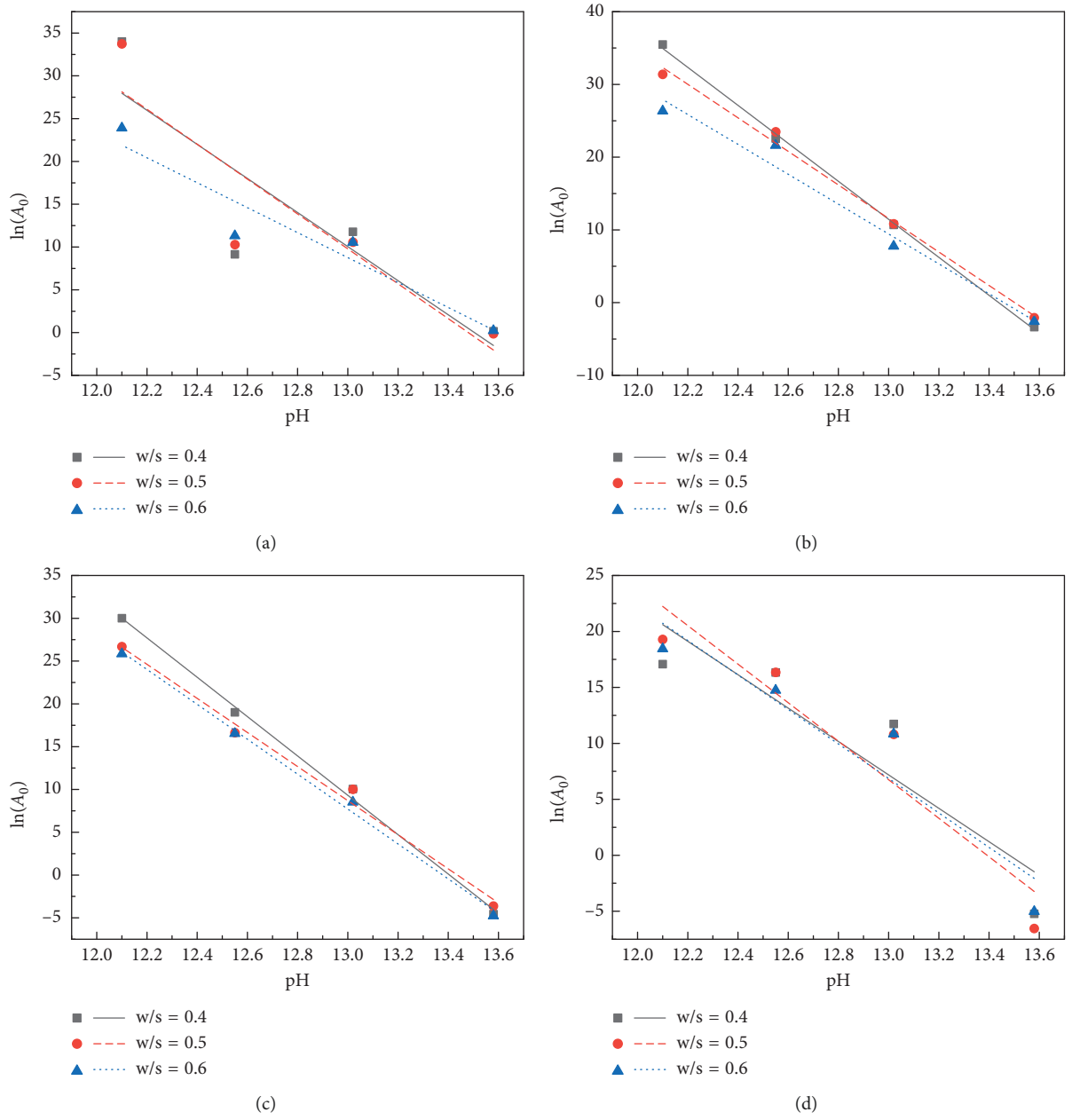

Figure 8: ln A_0 changes with pH at (a) 1 day, (b) 3 days, (c) 7 days, and (d) 14 days.

The effect of temperature and apparent activation energy on the rate of hydration can be seen from equation (8). The greater the apparent activation energy, the greater the influence of temperature on the hydration rate. That is to say, the greater the activation energy is, the more sensitive the hydration rate is to the change of temperature. In this study, the apparent activation energy decreases with the increase of pH. Therefore, in a low pH environment, increasing temperature is beneficial to hydration of slag. While in high pH solution, the apparent activation energy of slag is relatively small, and lowering temperature is more advantageous to slag hydration at this time.

When the activator solution pH is constant, the apparent activation energy E_a is known. The quantitative effect of temperature on slag hydration rate can be calculated by equation (9). This is of guiding significance for the production practice of AAS. According to this principle, the optimum hydration temperature of the slag and the initial pH of the solution can be selected to obtain the best hydration rate of AAS.

5. Conclusions

In this experiment, the hydration kinetics of AAS has been studied by the NEW content of the slag paste. According to the Arrhenius formula, the coupled effects of temperature and pH on the hydration rate and apparent activation energy are also obtained.

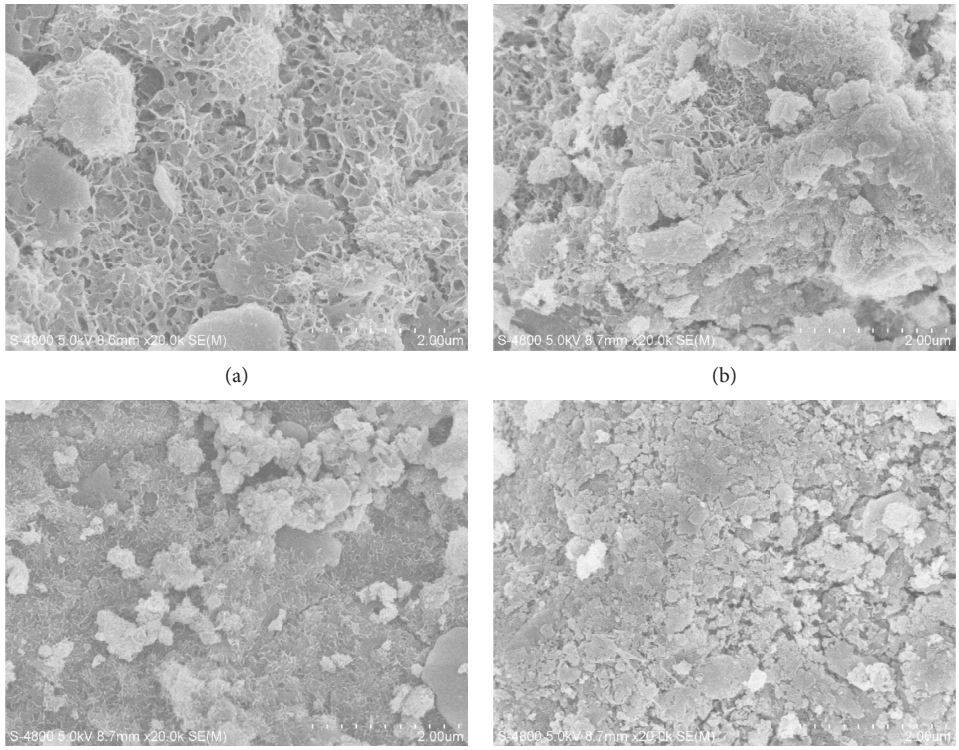

Figure 9: SEM images of slag particles with w/s = 0.4 in the solution pH 13.58. (a) 5°C, 1 day; (b) 35°C, 1 day; (c) 5°C, 14 days; (d) 35°C, 14 days.

(1) In the solution with pH ≤ 13.02, the NEW content of the slag paste increases with increasing of temperature and pH value. But in the high pH (pH = 13.58) solution, the NEW content at 20°C is always greater than that at 35°C throughout the curing ages. After 7 days, the NEW content at 5°C exceeds that at 20°C and 35°C, reaching the maximum.

(2) The early hydration degree of slag is significantly affected by temperature and pH. Increasing the temperature and pH of the activator solution can greatly shorten the activation time of the slag activity. However, in the high temperature and high pH environment (35°C, pH = 13.58), the hydration degree of slag growth is slow in the later stages.

(3) The apparent activation energy E_a of slag decreases with the increase of pH, and there is a good linear relationship between them. When pH is less than 13.02, increasing the temperature can accelerate the hydration rate of slag. However, under the condition of high pH, the hydration rate of slag is negatively correlated with temperature, which is related to the "shell forming" phenomenon of slag hydration.

(4) Through scanning electron microscopy (SEM) images, it is found that in the solution of pH 13.58, the surface of the slag particles at 5°C forms a net hydrated product structure. While at 35°C, a reacting shell is formed on the surface of the particles. This "shell forming" phenomenon inhibits the hydration reaction at the later stage of the slag, making the hydration rate of slag at 35°C lower than that at 5°C, so the apparent activation energy E_a and $\ln A_0$ appear as negative values.

(5) The greater the activation energy is, the more sensitive the hydration rate is to the change of temperature. According to this principle, the optimum hydration temperature of the slag and the initial pH of the solution can be selected to obtain the best reaction rate of the slag hydration. This is of guiding significance for the production practice of AAS.

Data Availability

The data used to support the findings of this study are available from the corresponding author upon request.

Conflicts of Interest

The authors declare that they have no conflicts of interest.

Acknowledgments

The authors would like to acknowledge the work supported by the National Key Research and Development Plan of China (Grant no. 2016YFC0401609), National Natural Science Foundation of China (Grant no. 51739008), and Fundamental Research Funds for the Central Universities (Grant no. 2018B13614).

References

[1] D. Zhang, S. Shi, C. Wang, X. Yang, L. Guo, and S. Xue, "Preparation of cementitious material using smelting slag and tailings and the solidification and leaching of Pb^{2+}," *Advances in Materials Science and Engineering*, vol. 2015, Article ID 352567, 7 pages, 2015.

[2] B. Lothenbach, K. Scrivener, and R. D. Hooton, "Supplementary cementitious materials," *Cement and Concrete Research*, vol. 41, no. 12, pp. 1244–1256, 2011.

[3] M. C. G. Juenger and R. Siddique, "Recent advances in understanding the role of supplementary cementitious materials in concrete," *Cement and Concrete Research*, vol. 78, pp. 71–80, 2015.

[4] F. Pacheco-Torgal, J. Castro-Gomes, and S. Jalali, "Alkali-activated binders: a review," *Construction and Building Materials*, vol. 22, no. 7, pp. 1305–1314, 2008.

[5] F. Sajedi and H. A. Razak, "Comparison of different methods for activation of ordinary Portland cement-slag mortars," *Construction and Building Materials*, vol. 25, no. 1, pp. 30–38, 2011.

[6] S.-D. Wang, K. L. Scrivener, and P. L. Pratt, "Factors affecting the strength of alkali-activated slag," *Cement and Concrete Research*, vol. 24, no. 6, pp. 1033–1043, 1994.

[7] M. Á. Sanjuán, E. Estévez, C. Argiz, and D. D. Barrio, "Effect of curing time on granulated blast-furnace slag cement mortars carbonation," *Cement and Concrete Composites*, vol. 90, pp. 257–265, 2018.

[8] S. Song, D. Sohn, H. M. Jennings et al., "Hydration of alkali-activated ground granulated blast furnace slag," *Journal of Materials Science*, vol. 35, no. 1, pp. 249–257, 2000.

[9] V. Živica, "Effects of type and dosage of alkaline activator and temperature on the properties of alkali-activated slag mixtures," *Construction and Building Materials*, vol. 21, no. 7, pp. 1463–1469, 2007.

[10] J. I. Escalante-Garcia, P. Castro-Borges, A. Gorokhovsky, and F. J. Rodriguez-Varela, "Portland cement-blast furnace slag mortars activated using waterglass: effect of temperature and alkali concentration," *Construction and Building Materials*, vol. 66, pp. 323–328, 2014.

[11] H. Zhou, X. Wu, Z. Xu, and M. Tang, "Kinetic study on hydration of alkali-activated slag," *Cement and Concrete Research*, vol. 23, no. 6, pp. 1253–1258, 1993.

[12] B. S. Gebregziabiher, R. Thomas, and S. Peethamparan, "Very early-age reaction kinetics and microstructural development in alkali-activated slag," *Cement and Concrete Composites*, vol. 55, pp. 91–102, 2015.

[13] Y.-M. Gu, Y.-H. Fang, D. You, Y.-F. Gong, and C.-H. Zhu, "Properties and microstructure of alkali-activated slag cement cured at below-and about-normal temperature," *Construction and Building Materials*, vol. 79, pp. 1–8, 2015.

[14] B. S. Gebregziabiher, R. J. Thomas, and S. Peethamparan, "Temperature and activator effect on early-age reaction kinetics of alkali-activated slag binders," *Construction and Building Materials*, vol. 113, pp. 783–793, 2016.

[15] J. I. Escalante, L. Y. Gómez, K. K. Johal, G. Mendoza, H. Mancha, and J. Méndez, "Reactivity of blast-furnace slag in Portland cement blends hydrated under different conditions," *Cement and Concrete Research*, vol. 31, no. 10, pp. 1403–1409, 2001.

[16] E. Altan and S. T. Erdoğan, "Alkali activation of a slag at ambient and elevated temperatures," *Cement and Concrete Composites*, vol. 34, no. 2, pp. 131–139, 2012.

[17] S. Glasstone, K. J. Laidler, and H. Eyring, *The Theory of Rate Processes: the Kinetics of Chemical Reactions, Viscosity, Diffusion, and Electrochemical Phenomena*, McGraw-Hill, New York, NY, USA, 1941.

[18] J. Zhou, X. Chen, and S. Chen, "Durability and service life prediction of GFRP bars embedded in concrete under acid environment," *Nuclear Engineering and Design*, vol. 241, no. 10, pp. 4095–4102, 2011.

[19] H. Mehdizadeh and E. Najafi Kani, "Rheology and apparent activation energy of alkali activated phosphorous slag," *Construction and Building Materials*, vol. 171, pp. 197–204, 2018.

[20] J. L. Poole, K. A. Riding, M. C. G. Juenger et al., "Effects of supplementary cementitious materials on apparent activation energy," *Journal of ASTM International*, vol. 7, no. 9, pp. 1–16, 2010.

[21] S.-D. Wang and K. L. Scrivener, "Hydration products of alkali activated slag cement," *Cement and Concrete Research*, vol. 25, no. 3, pp. 561–571, 1995.

[22] J. L. Provis, A. Palomo, and C. Shi, "Advances in understanding alkali-activated materials," *Cement and Concrete Research*, vol. 78, pp. 110–125, 2015.

[23] S. J. Barnett, M. N. Soutsos, S. G. Millard, and J. H. Bungey, "Strength development of mortars containing ground granulated blast-furnace slag: effect of curing temperature and determination of apparent activation energies," *Cement and Concrete Research*, vol. 36, no. 3, pp. 434–440, 2006.

[24] A. Fernández-Jiménez and F. Puertas, "Influencia de la concentración del activador sobre la cinética del proceso de activación alcalina de una escoria de alto horno," *Materiales de Construcción*, vol. 47, no. 246, pp. 31–42, 2010.

[25] H. Kada-Benameur, E. Wirquin, and B. Duthoit, "Determination of apparent activation energy of concrete by isothermal calorimetry," *Cement and Concrete Research*, vol. 30, no. 2, pp. 301–305, 2000.

[26] E. N. Kani, A. Allahverdi, and J. L. Provis, "Calorimetric study of geopolymer binders based on natural pozzolan," *Journal of Thermal Analysis and Calorimetry*, vol. 127, no. 3, pp. 2181–2190, 2017.

[27] H. Maghsoodloorad and A. Allahverdi, "Alkali-activation kinetics of phosphorus slag cement using compressive strength data," *Ceramics-Silikaty*, vol. 59, no. 3, pp. 250–260, 2015.

[28] V. Kocaba, E. Gallucci, and K. L. Scrivener, "Methods for determination of degree of reaction of slag in blended cement pastes," *Cement and Concrete Research*, vol. 42, no. 3, pp. 511–525, 2012.

[29] P. Y. Yan and F. H. Han, "Quantitative analysis of hydration degree of composite binder by image analysis and non-evaporable water content," *Journal of the Chinese Ceramic Society*, vol. 43, pp. 1331–1340, 2015.

[30] X. Chen and S. Wu, "Influence of water-to-cement ratio and curing period on pore structure of cement mortar," *Construction and Building Materials*, vol. 38, pp. 804–812, 2013.

[31] O. G. Rivera, W. R. Long, C. A. Weiss Jr. et al., "Effect of elevated temperature on alkali-activated geopolymeric binders compared to portland cement-based binders," *Cement and Concrete Research*, vol. 90, pp. 43–51, 2016.

[32] T. C. Powers, "Structure and physical properties of hardened Portland cement paste," *Journal of the American Ceramic Society*, vol. 41, no. 1, pp. 1–6, 1958.

[33] X. Chen, S. Wu, and J. Zhou, "Experimental study and analytical model for pore structure of hydrated cement paste," *Applied Clay Science*, vol. 101, pp. 159–167, 2014.

[34] Z. Tian, X. Wang, and X. Chen, "A new suction method for the measurement of pore size distribution of filter layer in permeable formwork," *Construction and Building Materials*, vol. 60, pp. 57–62, 2014.